ChemPubSoc Europe

DOI: 10.1002/chem.201304146

CHEMISTRY
A European Journal
Communication

Soft Porous Materials

Achieving a Rare Breathing Behavior in a Polycatenated 2D to 3D Net through a Pillar-Ligand Extension Strategy

Xiaoliang Zhao,[a, c] Fuling Liu,[c] Liangliang Zhang,[a] Di Sun,*[c] Rongming Wang,[a] Zhangfeng Ju,[b] Daqiang Yuan,*[b] and Daofeng Sun*[a, c]

Abstract: Through a pillar-ligand extension strategy, a rare breathing behavior in polycatenated 2D→3D nets has been achieved. Three variants exhibit interesting sorption properties that range from non-breathing to breathing behaviors, which is influenced by the angles between the pillars and the single honeycomb layers. The increase in pillar length does not lead to an increase in polycatenation multiplicity, which is controlled by the length of intralayer tripodal carboxylate. It also does not induce obviously expanded interlayer separations but occupies much more the free voids, and as a consequence, a smaller pore volume is obtained. This suggests that in 2D→3D polycatenated bilayer metal–organic frameworks, the porosity is not always enhanced by increasing the length of the interlayer pillars with the intralayer linker remaining unchanged.

Soft or flexible porous metal–organic frameworks (MOFs), which are also called dynamic frameworks, have received much attention owing to their potential applications in molecular recognition, selective gas adsorption/separation, or chemical sensing.[1] Compared to rigid porous MOFs, one of the most interesting phenomena in soft porous MOFs is their pronounced framework flexibility/dynamics under an external stimulus, such as pressure, temperature, guest solvents, or gas molecules.[2]

[a] X. Zhao,[+] L. Zhang, Prof. R. Wang, Prof. D. Sun
State Key Laboratory of Heavy Oil Processing
China University of Petroleum
College of Science, China University of Petroleum
Qingdao Shandong 266580 (P.R. China)
E-mail: dfsun@upc.edu.cn

[b] Z. Ju, Prof. D. Yuan
State Key Laboratory of Structural Chemistry, Fujian Institute of Research on the Structure of Matter, Chinese Academy of Sciences
Fujian, Fuzhou, 350002 (P.R. China)
E-mail: ydq@fjirsm.ac.cn

[c] X. Zhao,[+] F. Liu,[+] Prof. D. Sun, Prof. D. Sun
Key Laboratory of Colloid and Interface Chemistry, Ministry of Education
School of Chemistry and Chemical Engineering, Shandong University
No. 27, Shanda South Road, Jinan City, Shandong Province (P.R. China)
E-mail: dsun@sdu.edu.cn

[+] These authors contributed equally to this work.

Supporting information for this article (including experimental details) is available on the WWW under http://dx.doi.org/10.1002/chem.201304146.

The flexibility of MOFs or coordination polymers was first predicted by Kitagawa in 1998, when he classified porous coordination polymers into three categories: first, second, and third generations.[3] The prediction was illustrated by the observation of gate opening or breathing behaviors in 2D layered frameworks.[4] Recently, thanks to the development of supramolecular self-assembly and crystal engineering, a series of new type of soft porous MOFs have been synthesized and documented.[5] In particular, the breathing behaviors in MIL-53 and MIL-88 series, which sustain a cell unit contraction in volume upon hydration and the representative well-defined steps and hysteresis loop for gas sorption isotherms, were reported by Férey and co-workers.[6] Through the decoration of MOF-5 or designed synthesis of MOFs by introducing flexible substituents on the bdc-type linker, Cohen and Fischer independently reported the flexibility or breathing behaviors in rigid MOFs.[7,8] The shift between interpenetrated or partially interpenetrated nets to cause hysteretic gas sorption was recently reported by the groups of Chen,[9] Hupp,[10] Schröder,[11] and Kitagawa.[12] Most of the reported soft porous MOFs are limited to 2D layered frameworks, which can cause layer slide upon desolvation, or 3D porous frameworks, which can undergo reversible structural transitions between narrow pore (**np**) and large pore (**lp**) phases. However, the 3D pillared-bilayer MOFs generated from polycatenation of the 2D bilayers have been rarely investigated in adsorption, partially because they were usually considered to be less porous than stacked-type 2D networks due to the polycatenation.[13]

Recently, we reported a 3D porous MOFs based on the polycatenation among 2D bilayers.[14] Continuing our study, herein, we demonstrate, to the best of our knowledge, the first example of achieving breathing behavior in 2D→3D polycatenated pillared-bilayer MOFs through pillar-ligand extension strategy (Scheme 1). Our strategies were illustrated by design and synthesis of three polycatenated MOFs based on honeycomb bilayers, $[Zn_2(TMTA)(bpy)_{0.5}(H_2O)]_n$ (**1**·NO_3·2 DMF·H_2O), $[Zn_2(H_2O)_2$-$(TMTA)]_n[Zn_2(TMTA)\ (dpb)_{0.5}(H_2O)_2(dmf)]_n$ (**2**·2 NO_3·H_2O), and $[Zn_2(TMTA)(dpb)_{0.5}(H_2O)_2]_n$ (**3**·NO_3·8 DMF·3 H_2O) (H_3TMTA = 4,4′,4″-(2,4,6-trimethylbenzene-1,3,5-triyl)tribenzoic acid, bpy = 4,4′-bipyridine, dpb = 1,4-di(pyridin-4-yl)benzene). Interestingly, the elongation of the pillars not only enhanced the gas-uptake capability but also made the MOFs more flexible to achieve the breathing effect.

A comparison of structures of **1**–**3** is shown in Figure 1. The crystal structure of **1** has already been reported.[14] To construct a more porous material, 4,4-bipy was replaced by 1,4-di(pyri-

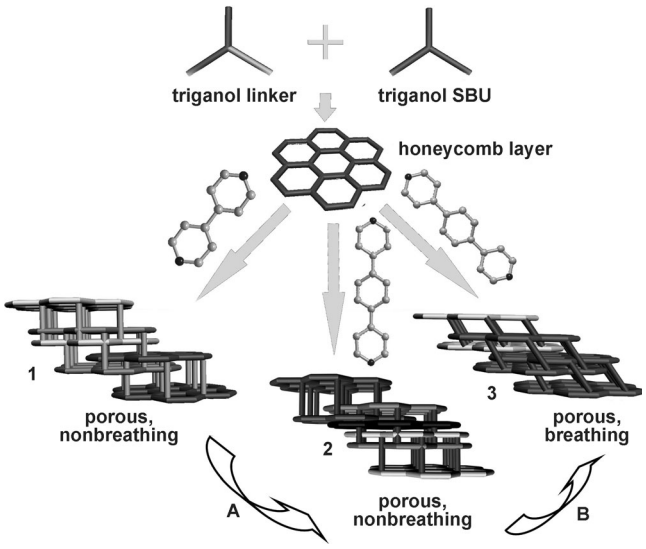

Scheme 1. Representation of the formation of single honeycomb layer and 3D MOFs from polycatenation. A) Pillar-ligand extension; B) Ligand ratio control to remove the single honeycomb layer.

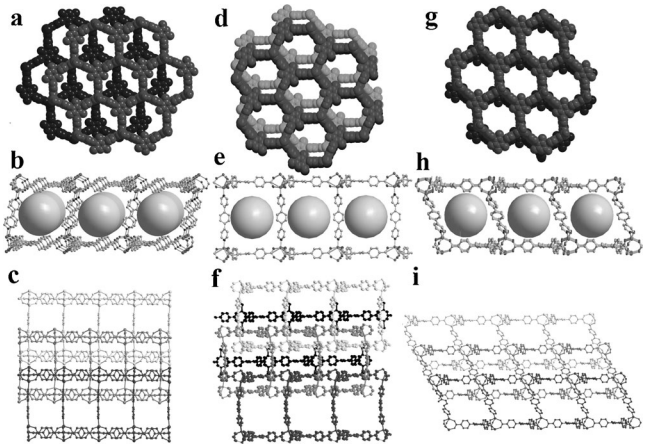

Figure 1. The 2D honeycomb layers for **1** (a), **2** (d), and **3** (g). The dipyridine-pillared 2D bilayer for **1** (b), **2** (e), and **3** (h). The 2D + 2D → 3D polycatenation of **1** (c), **2** (f), and **3** (i).[20]

din-4-yl)benzene (dpb) as the pillar in the assembly of **1** to give rise to complex **2**. There exist two units in the crystal structure of **2**: one is a 2D honeycomb single layer that is formed by TMTA as three-connected linkers connecting binuclear three-nodal zinc secondary building units (SBUs),[15] and the other is a 2D bilayer that is generated by dpb as pillars connecting two 2D honeycomb layers. In contrast to **1**, the 2D honeycomb single layers also interpenetrate with the 2D bilayers. As expected, the porosity of **2** increases slightly compared to **1** (see below). To remove the 2D honeycomb single layers to further improve the porosity, we decreased the ligand ratio of H_3TMTA in the assembly of **2**; complex **3** was isolated as colorless crystals. The interpenetrating fashion of **3** is quite similar to that in **1**, thus, the crystal structures for **1** and **3** are discussed together.

Both **1** and **3** are 2D→3D polycatenated MOFs based on honeycomb layers and rigid pillars. The rigid pillar ligands with different lengths extend the adjacent 2D layers to 2D bilayers (Figure 1 b, h) incorporating 1D uniform channels with cross sections of 14.4×16.3 and 17.3×18.0 Å^2 for **1** and **3**, respectively. The two honeycomb layers in the bilayer are parallel but with large relative displacement for **1**. This is not the same case for **3**, in which two layers are almost overlapped. Each bilayer contains two honeycomb layers belonging to two other bilayers. From the topology view, the binuclear [$Zn_2(COO)_3$] and the TMTA ligand can be seen as four-connected node and three-connected linker, so the overall 2D net is a 2-nodal (3,4)-connected bilayer with the Schläfli symbol {6^3}{6^6} and vertex symbol [6(2).6(2).6(2)] [6.6(2).6.6(2).6.6(2)] calculated by TOPOS software.[16] The 2D 6^3-***hcb*** single layer is very common in metal–organic structures; however, the 3, 4-connected bilayer structure reported here is, to our knowledge, still sparse.

Although the construction of polycatenated MOFs **1**–**3** are very similar, some structural differences between them should not be neglected. In **1** and **2**, the Zn^{II} ions that attach to the pillared linkers adopt tetrahedral coordination environments, whereas the Zn^{II} ions linked by the pillars in **3** are five-coordinate square-pyramidal geometries (Supporting Information, Figure S2). The pillared bpy and dpb ligands within the bilayer in **1**–**3** form angles of ca. 84, 89, and 52° with respect to the single layer, respectively (Figure 2). Although the structural differences between **1**, **2** and **3** are slight, the existence of different angles between the pillars and the honeycomb layers makes **1**, **2** and **3** possess quite different gas adsorption behaviors.

The total solvent-accessible volumes fraction of **1**, **2**, and **3** calculated by PLATON[11] are 40.7, 38.1, and 35.8%, respectively. To study the potential porosity of desolvated **1**, **2**, and **3**, sorption isotherms have been measured for N_2 at 77 K. Activation of samples involved the exchange of solvent molecules by methanol and dichloromethane, then vacuum-dried at 120 °C. The N_2 isotherms are shown in Figure 2. For **1** and **2**, the sorption of nitrogen at 77 K reaches near-saturation at low relative pressures ($P/P_0 < 0.05$) and thereafter increases very slowly up to 1 atm with total weight uptakes of 175 and 215 cm^3 g^{-1}, respectively. There is no significant hysteresis between sorption and desorption traces. With an approximation based on a monolayer condensation of adsorbed N_2 molecules on a uniform surface, the sorption isotherms were fitted to a Langmuir

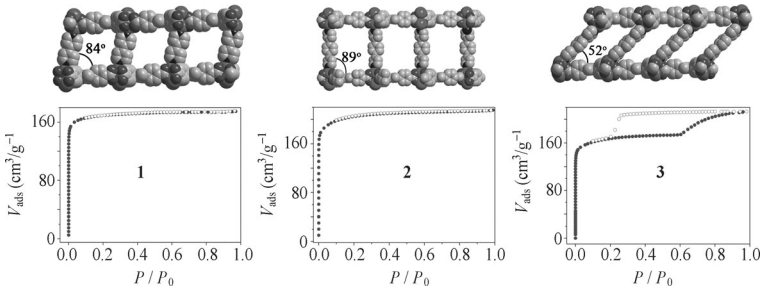

Figure 2. The angles between the pillars and the honeycomb layers in **1**–**3** (upper), and N_2 adsorption isotherms for **1**–**3** (bottom): ● adsorption, ○ desorption.

equation and gave surface areas of 747 and 925 $m^2 g^{-1}$ (677 and 788 $m^2 g^{-1}$ for BET model), respectively.

The most fascinating feature for **3** is a two-step adsorption process with that a profound desorption hysteresis was observed in both N_2 (77 K) and Ar (87 K) adsorption isotherms (Figure 2). For N_2 isotherm, the first step of the adsorption curve, in the range of $P/P_0 = 0.01–0.10$, shows a very fast uptake and the isotherm reaches its first plateau between the P/P_0 values 0.10 and 0.58, which resembles a typical type I isotherm. At higher pressures ($P/P_0 > 0.58$), the second step of the adsorption happens and its maximum adsorption amount reaches 214 $cm^3 g^{-1}$ at $P/P_0 \approx 1.0$. During the desorption process, the adsorbed N_2 could stay in the pores at the range of 1.0–0.26, and the first step of desorption was obviously observed below a pressure of $P/P_0 = 0.26$. The desorption curve does not retrace the adsorption curve until P/P_0 reaches 0.20, and at that point the hysteresis loop closes with the remaining N_2 of 170 $cm^3 g^{-1}$. The second desorption occurred dramatically from $P/P_0 = 0.02$ to $P/P_0 \approx 0$.

The broad hysteresis loops usually associated with the existence of mesopores; however, the hysteresis loops in **3** cannot be simply explained as mesopores. As for the mesoporous materials, the lower closure point in desorption branch occurs at relative pressure $P/P_0 \approx 0.42$ for N_2 at 77 K.[17] It is obvious that the lower closure point of $P/P_0 = 0.20$ is much lower than 0.42, which reflects that other reasons cause the unique hysteresis in **3**. The pore volume calculated from the first adsorption plateau is 0.26 $cm^3 g^{-1}$, which is very close to the theoretical value of 0.23 $cm^3 g^{-1}$ predicted from crystal structure. However, the total pore volume of 0.33 $cm^3 g^{-1}$ is significantly larger than the theoretical one. Therefore, the second step of gas uptake may be attributed to the expanded intermediate form, which possesses an increased pore volume owing to the expansion of the interlayer distance upon adsorption.[18]

As indicated by above structural analysis and gas adsorption measurements, the angles between the pillars and the single honeycomb layers in **3** are significantly shorter than those in **1** and **2**, which make the framework **3** more flexible, so its interlayer distances may be expanded under the pressure stimuli, accompanying the less oblique posture of dpt ligand appeared. The displacement of two single layers in one bilayer brings the enlargement of the pores.

Although many MOFs showing a structural change by external stimuli have been reported, only a few show a definite stepwise sorption isotherm related to a breathing effect.[19] Compared to previously reported MOFs with breathing effect, in our case, the structure of 2D layer is eternal owing to the fixed structure of TMTA, but the change of the pillared ligands give us surprising results. The pillaring roles of the rigid bipyridyl ligand is very important and diverse, it not only fixes the neighboring layers with an appropriate distance and prevent the clogging of micropores, but also could modulate itself to response to the external stimuli (Figure 3). As such, the length of the pillared ligand becomes an effective strategy to modulate the adsorption properties in this work.

In conclusion, through a pillar-ligand extension strategy, a rare breathing behavior in polycatenated 2D→3D nets has been successfully achieved. Structures **1**, **2**, and **3** exhibit interesting sorption properties ranging from non-breathing to breathing behaviors influenced by the angles between the pillars and the single honeycomb layers. Comparing the structures of **1** and **3**, the increase in pillar length does not lead to increase in polycatenation multiplicity, which is controlled by the length of intralayer tripodal carboxylate. Surprisingly, it also does not induce obviously expanded interlayer separations but occupies much more free voids; as a consequence, a smaller pore volume is obtained. This suggests that in 2D→3D polycatenated bilayer MOFs, the porosity is not always enhanced by increasing the length of the interlayer pillars with the intralayer linker remaining unchanged. Structural alteration arising from the different pillar ligands and results of gas sorption experiments may be useful in designing a new metal–organic porous material for gas storage applications.

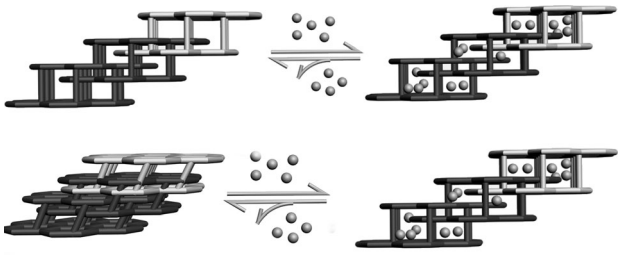

Figure 3. The possible mechanism for **1** (upper) and **3** (bottom) upon the stimuli of gas molecules.

Acknowledgements

This work was supported by the NSFC (Grant 90922014, 21001115, 21271117), NCET-11–0309 and the Shandong Natural Science Fund for Distinguished Young Scholars (JQ201003), Independent Innovation Foundation of Shandong University (2011GN030), and the Fundamental Research Funds for the Central Universities (13CX05010A).

Keywords: hysteresis · polycatenation · metal–organic frameworks · soft porous materials

[1] a) Y. Sakata, S. Furukawa, M. Kondo, K. Hirai, N. Horike, Y. Takashima, H. Uehara, N. Louvain, M. Meilikhov, T. Tsuruoka, S. Isoda, W. Kosaka, O. Sakata, S. Kitagawa, *Science* **2013**, *339*, 193–196; b) S. Horike, S. Shimomura, S. Kitagawa, *Nat. Chem.* **2009**, *1*, 695–704; c) G. Férey, C. Serre, *Chem. Soc. Rev.* **2009**, *38*, 1380–1399; d) S. Kitagawa, K. Uemura, *Chem. Soc. Rev.* **2005**, *34*, 109–119.

[2] a) C. Serre, C. Mellot-Draznieks, S. Surblé, N. Audebrand, Y. Filinchuk, G. Férey, *Science* **2007**, *315*, 1828–1831; b) J. Seo, C. Bonneau, R. Matsuda, M. Takata, S. Kitagawa, *J. Am. Chem. Soc.* **2011**, *133*, 9005–9013.

[3] S. Kitagawa, M. Kondo, *Bull. Chem. Soc. Jpn.* **1998**, *71*, 1739–1753.

[4] a) D. Tanaka, K. Nakagawa, M. Higuchi, S. Horike, Y. Kubota, T. C. Kobayashi, M. Takata, S. Kitagawa, *Angew. Chem.* **2008**, *120*, 3978–3982; *Angew. Chem. Int. Ed.* **2008**, *47*, 3914–3918; b) A. Kondo, H. Noguchi, L. Carlucci, D. M. Proserpio, G. Ciani, H. Kajiro, T. Ohba, H. Kanoh, K. Kaneko, *J. Am. Chem. Soc.* **2007**, *129*, 12362–12363.

[5] a) B. Mu, F. Li, Y. G. Huang, K. S. Walton, *J. Mater. Chem.* **2012**, *22*, 10172–10178; b) S. J. Wang, L. Li, J. Y. Zhang, X. C. Yuan, C. Y. Su, *J. Mater. Chem.* **2011**, *21*, 7098–7104; c) S. Bureekaew, H. Sato, R. Matsuda, Y. Kubota, R. Hirose, J. Kim, K. Kato, M. Takata, S. Kitagawa, *Angew.*

Chem. **2010**, *122*, 7826 – 7830; *Angew. Chem. Int. Ed.* **2010**, *49*, 7660 – 7664; d) L.-H. Xie, M. P. Suh, *Chem. Eur. J.* **2011**, *17*, 13653 – 13656; e) P. Kanoo, K. L. Gurunatha, T. K. Maji, *J. Mater. Chem.* **2010**, *20*, 1322 – 1331; f) A. M. Walker, B. Civalleri, B. Slater, C. Mellot-Draznieks, F. Cora, C. M. Zicovich-Wilson, G. Roman-Perez, J. M. Soler, J. D. Gale, *Angew. Chem.* **2010**, *122*, 7663 – 7665; *Angew. Chem. Int. Ed.* **2010**, *49*, 7501 – 7503; g) P. K. Thallapally, J. Tian, M. R. Kishan, C. A. Fernandez, S. J. Dalgarno, P. B. McGrail, J. E. Warren, J. L. Atwood, *J. Am. Chem. Soc.* **2008**, *130*, 16842 – 16843; h) J. S. Grosch, F. Paesani, *J. Am. Chem. Soc.* **2012**, *134*, 4207 – 4215.

[6] a) C. Serre, F. Millange, C. Thouvenot, M. Noguès, G. Marsolier, D. Louër, G. Férey, *J. Am. Chem. Soc.* **2002**, *124*, 13519 – 13526; b) P. Horcajada, F. Salles, S. Wuttke, T. Devic, D. Heurtaux, G. Maurin, A. Vimont, M. Daturi, O. David, E. Magnier, N. Stock, Y. Filinchuk, D. Popov, C. Riekel, G. Férey, C. Serre, *J. Am. Chem. Soc.* **2011**, *133*, 17839 – 17847.

[7] Z. Q. Wang, S. M. Cohen, *J. Am. Chem. Soc.* **2009**, *131*, 16675 – 16677.

[8] a) S. Henke, A. Schneemann, A. Wutscher, R. A. Fischer, *J. Am. Chem. Soc.* **2012**, *134*, 9464 – 9474; b) S. Henke, R. Schmid, J. Grunwaldt, R. A. Fischer, *Chem. Eur. J.* **2010**, *16*, 14296 – 14306.

[9] B. L. Chen, C. D. Liang, J. Yang, D. S. Contreras, Y. L. Clancy, E. B. Lobkovsky, O. M. Yaghi, S. Dai, *Angew. Chem.* **2006**, *118*, 1418 – 1421; *Angew. Chem. Int. Ed.* **2006**, *45*, 1390 – 1393.

[10] K. L. Mulfort, O. K. Farha, C. D. Malliakas, M. G. Kanatzidis, J. T. Hupp, *Chem. Eur. J.* **2010**, *16*, 276 – 281.

[11] S. H. Yang, X. Lin, W. Lewis, M. Suyetin, E. Bichoutskaia, J. E. Parker, C. C. Tang, D. R. Allan, P. J. Rizkallah, P. Hubberstey, N. R. Champness, K. M. Thomas, A. J. Blake, M. Schröder, *Nat. Mater.* **2012**, *11*, 710 – 716.

[12] T. K. Maji, R. Matsuda, S. Kitagawa, *Nat. Mater.* **2007**, *6*, 142 – 148.

[13] a) C.-Y. Su, A. M. Goforth, M. D. Smith, H.-C. Zur Loye, *Chem. Commun.* **2004**, 2158 – 2159; b) X. Q. Lv, Y. Q. Qiao, J. R. He, M. Pan, B. S. Kang, C. Y. Su, *Cryst. Growth Des.* **2006**, *6*, 1910 – 1914.

[14] X. L. Zhao, J. M. Dou, D. Sun, P. P. Cui, D. F. Sun, Q. Y. Wu, *Dalton Trans.* **2012**, *41*, 1928 – 1930.

[15] S. Vagin, A. K. Ott, B. Rieger, *Chem. Ing. Tech.* **2007**, *79*, 767 – 780.

[16] V. A. Blatov, TOPOS, A Multipurpose Crystallochemical Analysis with the Package, Samara State University, Russia, **2004**.

[17] K. S. W. Sing, D. H. Everett, R. A. W. Haul, L. Moscou, R. A. Pierotti, J. Rouquerol, T. Siemieniewska, *Pure Appl. Chem.* **1985**, *57*, 603 – 619.

[18] P. Kanoo, G. Mostafa, R. Matsuda, S. Kitagawa, T. K. Maji, *Chem. Commun.* **2011**, *47*, 8106 – 8108.

[19] a) J. Seo, R. Matsuda, H. Sakamoto, C. Bonneau, S. Kitagawa, *J. Am. Chem. Soc.* **2009**, *131*, 12792 – 12800; b) C. Serre, S. Bourrelly, A. Vimont, N. A. Ramsahye, G. Maurin, P. L. Llewellyn, M. Daturi, Y. Filinchuk, O. Leynaud, P. Barnes, G. Férey, *Adv. Mater.* **2007**, *19*, 2246 – 2251.

[20] CCDC 831821 (**1**), CCDC 956596 (**2**), and CCDC 891972 (**3**) contain the supplementary crystallographic data for this paper. These data can be obtained free of charge from the Cambridge Crystallographic Data Centre via www.ccdc.cam.ac.uk/data_request/cif.

Received: November 4, 2013
Published online on December 11, 2013